Glu-320 and Asp-323 Are Determinants of the CYP4A1 Hydroxylation Regiospecificity and Resistance to Inactivation by 1-Aminobenzotriazole†

Elizabeth A. Dierks, S. Christopher Davis, and Paul R. Ortiz de Montellano*

Department of Pharmaceutical Chemistry, University of California, San Francisco, California 94143-0446

Received October 3, 1997; Revised Manuscript Received November 21, 1997

ABSTRACT: Little information is available on the active site structure of the CYP4A family of enzymes or the mechanism by which their ω-hydroxylation regiospecificity is enforced. We report here that the E320A, D323E, and E320/D323E mutations decrease the catalytic rate of CYP4A1 ~5-fold and cause up to a 10-fold shift from ω- to (ω−1)-hydroxylation. The decreased catalytic rate is due to an increase in the uncoupled reduction of molecular oxygen. Tighter binding of 1- and 4-substituted imidazoles to the double mutant than to the other proteins suggests that its active site is less constrained. The reaction of these proteins with phenyldiazene causes heme degradation without the detectable formation of a phenyl−iron complex. CYP4A1 and its E320A mutant are not inactivated by 1-aminobenzotriazole (1-ABT), but the D323E and E320A/D323E mutants are inactivated. The resistance of purified CYP4A1 to inactivation by 1-ABT is surprising in view of the fact that 1-ABT causes the loss of the ω-hydroxylase activity both in microsomal preparations and in vivo. Collectively, the results establish that Glu-320, and particularly Asp-323, help to define the active site dimensions, the degree of coupled versus uncoupled turnover, the ω- versus (ω−1)-hydroxylation regiospecificity, and the susceptibility to inactivation by mechanism-based inhibitors. Furthermore, they provide experimental evidence for a structural analogy between the CYP4A1 and $P450_{BM-3}$ active sites.

The CYP4A family of cytochrome P450 enzymes catalyzes the ω- and (ω−1)-hydroxylation of fatty acids (*1*, *2*). The four CYP4A enzymes present in rat liver and kidney, CYP4A1, CYP4A2, CYP4A3, and CYP4A8, exhibit 72−96% amino acid sequence similarity (*3*, *4*). The first three enzymes are present in rat liver and are induced by clofibrate (*3*), and all four enzymes are either present constitutively in the kidney (CYP4A2, CYP4A8) or can be induced in that organ by clofibrate (*3*−*5*). Although several other enzymes, notably CYP2E1 (*6*, *7*) and CYP2C2 (*8*), catalyze the ω−1 hydroxylation of fatty acids, the CYP4A enzymes are unique in their high specificity for ω-hydroxylation. Of the four rat fatty acid ω-hydroxylases, the best characterized is CYP4A1, which catalyzes the ω- and (ω−1)-hydroxylation of lauric acid in a 20:1 ratio, respectively (*9*; vide infra). The predominant ω-hydroxylase in human liver and kidney is CYP4A11, which exhibits properties similar to those of rat CYP4A1 (*10*).

We argued earlier that the ω-regiospecificity of the CYP4A enzymes requires specific intervention of the enzyme in the hydroxylation process because the primary C−H bonds of the terminal methyl group are stronger (i.e., less reactive) than the secondary C−H bonds of the ω−1 methylene group (*11*). Thus, the default regiochemistry for fatty acid oxidation by enzymes not specifically designed to promote ω-hydroxylation is (ω−1)-hydroxylation or the hydroxylation of methylene groups farther into the fatty acid chain (*6*−*8*). The structural basis for the ω-hydroxylation specificity of CYP4A enzymes is not known, however. The only cytochrome P450 crystal structures currently available are for the soluble bacterial enzymes $P450_{cam}$ (CYP101) (*12*), $P450_{terp}$ (CYP108) (*13*), $P450_{BM-3}$ (CYP102) (*14*), and $P450_{eryF}$ (CYP107) (*15*). No crystal structure is available for a eukaryotic, membrane-bound P450 enzyme such as CYP4A1. The closest structurally defined model for the CYP4A enzymes is $P450_{BM-3}$, an enzyme that hydroxylates fatty acids at the ω−1, ω−2, and ω−3, but not ω, positions (*16*). A crystal structure of substrate-bound $P450_{BM-3}$ indicates that the fatty acid lies in a long channel, with the carboxylic acid group hydrogen bonded to Tyr-51 and Arg-47 near the mouth of the channel (*17*). The hydrocarbon tail extends into the heme[1] crevice but curves away from the heme iron atom (Figure 1), in part because Phe-87 is positioned so that it interferes with approach of the ω-terminal carbon to the iron atom (*17*). Anchoring the two ends of the fatty acid allows the fatty acid chain sufficient mobility to permit the enzyme to bind and oxidize fatty acids of

† This work was supported by National Institutes of Health Grant GM25515, with support for the spectrophotometry core facility of the Liver Center (R. Ockner, Director) by Grant 5 P30 DK26743.

* To whom correspondence should be addressed. FAX: (415) 502-4728. E-mail: ortiz@cgl.ucsf.edu.

[1] Abbreviations: heme, iron protoporphyrin IX regardless of the iron oxidation or ligation state; E320A, the E320A CYP4A1 mutant; D323E, the D323E CYP4A1 mutant; E320A/D323E, the E320A/D323E CYP4A1 mutant; 1-ABT, 1-aminobenzotriazole.

S0006-2960(97)02458-6 CCC: $15.00
Published on Web 01/30/1998

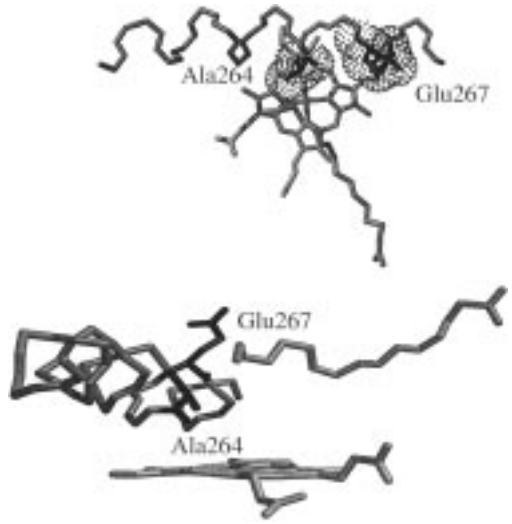

FIGURE 1: I-helix domain of the $P450_{BM-3}$ crystal structure that, on the basis of sequence alignments, corresponds to the region mutated in CYP4A1: (upper) top view and (lower) side view (*17*). The heme group and the palmitoleic acid ligand are also shown. The two labeled residues, Ala-264 and Glu-267, are the residues in $P450_{BM-3}$ that correspond to Glu-320 and Asp-323 in CYP4A1. The E320A and D323E mutations convert the CYP4A1 residues to the residues found in $P450_{BM-3}$.

different lengths. Interestingly, mutation of Phe-87 to an alanine alters the enzymatic regiospecificity so as to favor ω- over ($\omega-1$)- hydroxylation (*18*). The detailed structural changes responsible for this mutation-dependent shift in regiospecificity are unclear, however, because the enzyme−substrate complex undergoes a major conformational change when the iron is reduced from the ferric to the ferrous state in the first step of catalytic turnover (*19*).

The substrate specificity of CYP4A1 for fatty acid chains of different lengths suggests a possible similarity in the binding of fatty acids to CYP4A1 and $P450_{BM-3}$. Indeed, Hanzlik and co-workers have found that the affinity of the enzyme for fatty acid analogues with a terminal imidazole function depends on the fatty acid chain length, whereas the chain length specificity is lost if the carboxyl group is replaced by a nonpolar functional group (*20*). Indirect evidence suggests that the active sites of the CYP4A enzymes are highly constrained and that their ω-specificity is achieved, at least in part, by limiting access of the fatty acid terminus to the iron-linked oxidizing species (*11*). Thus, rat liver microsomal fatty acid ω-hydroxylation is not supported by cumene hydroperoxide but is supported to a small extent by H_2O_2 (*21*, *22*), which suggests that peroxide access to the heme iron atom is limited. Inactivation of the enzyme by 10-undecynoic acid, a fatty acid with a terminal acetylenic group, involves transfer of the activated oxygen to the terminal carbon, leading to formation of the ketene metabolite that alkylates the protein (*11*). This contrasts with the inactivation by acetylenes of many other P450 enzymes, which involves transfer of the activated oxygen to the $\omega-1$ triple-bond carbon and results in N-alkylation of the prosthetic heme group (*23*). The topology of the enzyme is not simple, however, because Bambal and Hanzlik have found that the enzyme tolerates significant steric bulk at the $\omega-1$ position, as illustrated by the ω-hydroxylation of substrates with a terminal function as large as a *tert*-butyl group (*24*).

1-Aminobenzotriazole (1-ABT) is a mechanism-based inhibitor that inactivates the P450-dependent fatty acid ω-hydroxylase activities both in microsomal preparations (*25*) and in vivo (*22*, *26*−*28*). This inactivation by 1-ABT is surprising because it is a bulky aromatic compound that might not be expected to be oxidized by the CYP4A family of enzymes. The inactivation of P450 enzymes by 1-ABT involves the catalytic formation of benzyne which either adds across two nitrogens of the prosthetic heme group to give a bridged heme adduct (*29*, *30*) or in some instances binds covalently to the protein (*31*). However, no investigation has been carried out of the inactivation of any purified CYP4A enzyme by 1-ABT, and the mechanism of the inactivation of these enzymes is unknown.

We report here mutation of two residues in CYP4A1 that increase substrate access to the active site, increase uncoupled enzyme turnover, and cause an order of magnitude change in the ω- vs ($\omega-1$)-regiospecificity of the enzyme. The increased active site access, however, is not sufficient to make the iron susceptible to reaction with phenyldiazene, a topological probe that reacts with the iron of P450 enzymes (*32*). Furthermore, we demonstrate that pure CYP4A1 is not directly inactivated by 1-ABT, but that one of the active site mutations makes it susceptible to such inactivation.

EXPERIMENTAL PROCEDURES

Materials. The pAlter kit and IPTG were purchased from Promega. Ampicillin, KP_i, imidazole, δ-aminolevulinic acid, glycerol, lysozyme, dilauroylphosphatidylcholine, glutathione, catalase, NADPH, lauric acid, 12-hydroxylauric acid, and 1-ABT were obtained from Sigma. Tris, EDTA, sodium cholate, NaCl, $MgCl_2$, H_2SO_4, and MeOH were purchased from Fisher. Emulgen 913 was a gift of Kao Chemicals. Tryptone and yeast extract were from Difco Laboratories. Substituted imidazoles were from Aldrich. ^{14}C-Lauric acid (55 mCi/mmol) was purchased from American Radiolabeled Chemicals, Inc. The CYP4A1 cDNA was kindly provided by R. Estabrook (University of Texas Southwestern Medical Center) (*33*), and the human NADPH-cytochrome P450 reductase and cytochrome b_5 cDNAs were provided by Stephen M. Black (University of California, San Francisco). The pCWori vector was a gift from Robert Fletterick (University of California, San Francisco) (*34*).

Mutations in CYP4A1. A sequence encoding a six-His tail was added to the CYP4A1 gene via PCR. The primers introduced an *Nde*I site, an *Xba*I site, and a carboxy-terminal six-His tail: primer 1 (amino terminus, 5′−3′), AGTCCAGTCCAGCATATGGCTCTGTTATTAGCAGTTTTTCTGCTTCTGCTGCTG; primer 2 (carboxy terminus, 5′−3′), AGTCCAGTCCAGTCTAGATTAGTGATGGTGATGATGATGTCCGTGGAGCTTCTTGAGATA. E320A and D323E were made by single mutations of the poly(His)-tailed P4504A1, and E320A/D323E was made by a single mutation of D323E using the pAlter plasmid and kit: primer 3 (E320A, 5′−3′) CATTTATGTTCGCGGGTCATGACAC; primer 4 (D323E, 5′−3′), CGAGGGTCATGAGACCACAGCCAGT; primer 5 (E320A/D323E, 5′−3′), CATTTATGTTCGCGGGTCATGAGAC. The genes were ligated into pCWori for expression.

Expression of CYP4A1, E320A, D323E, and E320A/D323E. The pCWori plasmid containing the appropriate

CYP4A1 cDNA (CYP4A1, E320A, D323E, or E320A/D323E) was transformed into *Escherichia coli* XL-1 Blue (Stratagene), and a single colony was grown overnight in 2 × YT with 200 μg/mL of ampicillin. One liter of terrific broth with 200 mg/L ampicillin was inoculated with 2 mL of the saturated overnight culture and grown at 37 °C to an OD_{600} of 0.1. At this point, 80 mg/L of δ-aminolevulinic acid was added and the flasks were returned to the incubator. Once the flasks reached an OD_{600} of 0.5−0.6, they were induced with 1 mM IPTG and cooled to 28 °C. The cells were grown for an additional 18 h.

Purification of CYP4A1, E320A, D323E, and E320A/D323E. To purify the proteins, the cells were harvested by centrifugation at 4000*g* for 20 min. The pellet was resuspended in 100 mM Tris (pH 7.8) containing 0.1 mM EDTA and 20% glycerol, and the suspension was stirred with lysozyme for 1 h at 4 °C. The cell suspension was centrifuged at 4000*g* for 30 min. The cells were resuspended in 10 mM Tris (pH 7.4) containing 0.1 mM EDTA, and the suspension on ice was sonicated for 7 min (1 min on, 1 min off, 50% power). The cell debris and unbroken cells were removed by centrifugation at 12000*g* for 10 min. The supernatant was centrifuged at 100000*g* for 1 h to pellet the cell membranes. The membranes were resuspended in 20 mM KP_i (pH 7.4) containing 20% glycerol, and Emulgen 913 was slowly added to a final concentration of 1% while being stirred gently at 25 °C for 1 h to solubilize the CYP4A1. The nonsolubilized protein was removed by centrifugation at 100000*g* for 1 h. The supernatant was frozen in liquid N_2 and stored at −70 °C.

The solubilized CYP4A1 was thawed and stirred gently for 1 h at 4 °C with 5 mL of Ni^{2+}-NTA-agarose (Novagen) that had been equilibrated previously with 20 mM Tris (pH 8.0) containing 1 M NaCl, 5 mM imidazole, 0.02% cholate, and 20% glycerol. The resin−protein slurry was poured into a 2.5-cm-diameter column. The resin was then washed with 10 volumes of 20 mM Tris (pH 8.0) containing 1 M NaCl, 5 mM imidazole, 0.02% cholate, and 20% glycerol, followed by 8 volumes of 20 mM Tris (pH 8.0) containing 1 M NaCl, 30 mM imidazole, 0.02% cholate, and 20% glycerol. The CYP4A1 was eluted by washing the column with 10 volumes of 20 mM Tris (pH 8.0) containing 0.5 M imidazole, 0.5 M NaCl, 0.02% cholate, and 20% glycerol. The imidazole was removed by desalting aliquots of CYP4A1 just prior to use on a Pharmacia PD-10 column which was equilibrated with 20 mM KP_i (pH 7.4) containing 0.02% cholate and 20% glycerol. The P450 content was determined using the method of Omura and Sato (*35*).

Expression and Purification of Human NADPH-P450 Reductase. The plasmid pET22b containing the human NADPH-P450 reductase gene was transformed into Novagen BL21 $pLys^s$ *E. coli* cells, and a single colony was grown overnight in 2 × YT containing 200 μg/mL of ampicillin. One liter of terrific broth containing 200 mg/L of ampicillin was inoculated with 1.5 mL of the saturated overnight culture and grown at 37 °C. Once the cells reached an OD_{600} of 0.4, the temperature was reduced to 22 °C and the flasks were induced with 0.4 mM IPTG. The cells were grown for an additional 16 h.

The cells were harvested by centrifugation at 4000*g* for 20 min and lysed with stirring for 1 h at 4 °C in 100 mM Tris (pH 7.8) containing 1 mM EDTA, 1 mM PMSF, 1 mg/L pepstatin, 10 mg/L leupeptin, 0.1 mg/L antipain, 20% glycerol, and 50 mg/mL lysozyme. The cells were then sonicated on ice 7 min (1 min on, 1 min off, 50% power), and the cell debris was removed by centrifugation at 12000*g* for 10 min. The supernatant was centrifuged at 100000*g* for 1 h to pellet the cell membranes. The reductase was solubilized by stirring 1 h at 4 °C in 20 mM KP_i (pH 7.4) containing 20% glycerol, 0.1 mM EDTA, 1 mM PMSF, 1 mg/L pepstatin, 10 mg/L leupeptin, 0.1 mg/L antipain, and 0.2% Lubrol PX (Sigma). The nonsolubilized proteins were removed by centrifugation at 100000*g* for 1 h.

The supernatant was loaded onto a 10-mL 2′,5′-ADP−Sepharose column that was equilibrated with 20 mM KP_i (pH 7.4) containing 20% glycerol and 0.1 mM EDTA. The column was washed with 5 volumes of 20 mM KP_i containing 20% glycerol and 0.1 mM EDTA, followed sequentially by 10 volumes of 300 mM KP_i containing 20% glycerol and 0.1 mM EDTA, and 5 volumes of 20 mM KP_i containing 20% glycerol, 0.1 mM EDTA, and 0.15% cholate. The reductase was eluted with 20 mM KP_i containing 20% glycerol, 0.1 mM EDTA, 0.15% cholate, and 5 mM 2′-AMP. The cholate and 2′-AMP were removed from the reductase by dilution with 20 mM KP_i containing 5% glycerol and concentration in an Amicon ultrafiltration cell.

Expression and Purification of Cytochrome b_5. Cytochrome b_5 was expressed and prepared by an adaptation of the method of Estabrook (*36*). Imidazole was removed by dilution with 20 mM Kp_i (pH 7.4) containing 0.02% cholate and 5% glycerol, followed by concentration in an Amicon ultrafiltration cell.

Measurement of CYP4A1 Hydroxylation Activity. CYP4A1 ω-hydroxylase activity was measured by a modification of the method of Ortiz de Montellano and Reich (*25*). The enzyme reaction was set up in a disposable glass centrifuge tube (5 mL): 10 μg of dilauroylphosphatidylcholine, 0.1 mg of sodium cholate, 25 pmol of CYP4A1, 250 pmol of reductase, 25 pmol of b_5, 1.5 μmol of glutathione, and catalase were gently mixed together and incubated for 10 min at room temperature. Next 50 mM KP_i (pH 7.5) containing 15 μmol of $MgCl_2$ and ^{14}C-lauric acid (2.5 μCi from a 60 mM mixture of 5:1 unlabeled to ^{14}C-labeled lauric acid, final concentration of lauric acid in assay 600 μM) was added to the CYP4A1 mixture to a final volume of 490 μL prior to a 5-min incubation at 37 °C. Finally 10 μL of 100 mM NADPH was added to start the reaction, which was carried out at 37 °C. The reaction was quenched by addition of 0.4 mL of 10% H_2SO_4. The samples were diluted with 0.5 mL of doubly distilled H_2O and then extracted twice with 1 mL of diethyl ether. The organic extract was mixed with excess diazomethane and allowed to evaporate to dryness overnight in a hood at room temperature. The lauric acid derivatives were redissolved in 0.3 mL of MeOH, and 50 μL was injected onto an Alltech Econosil C_{18} 5-μm reverse-phase column equilibrated with 80% MeOH−20% H_2O and coupled to a Beckman System Gold 166 UV monitor and a Packard Radiomatic Flow-One model 515 radioisotope detector. The 11- and 12-hydroxylauric acid methyl esters and lauric acid methyl ester were separated at a flow rate of 0.5 mL/min with a 20-min 80% MeOH-20% H_2O wash, a 5-min linear gradient to 100% MeOH, and a 30-min wash with 100% MeOH. 11-Hydroxylauric acid eluted at 19.5

min, 12-hydroxylauric acid at 21 min, and lauric acid at 49 min.

Reaction of CYP4A1, E320A, D323E, and E320A/D323E with 1-ABT. Samples were prepared for hydroxylation activity assay as above except that the lauric acid was added last after the samples were preincubated for 10 min at 37 °C with 10 mM 1-ABT in the presence of NADPH. Addition of lauric acid began the hydroxylation assay.

Measurement of NADPH Consumption. Samples of CYP4A1, E320A, D323E, and E320A/D323E were prepared for hydroxylation activity assay in a 0.1-cm cuvette as above except that only unlabeled lauric acid was used in the assay. The change in absorbance at 340 nm was monitored over 30 min at 37 °C.

Reaction of CYP4A1, E320A, D323E, E320A/D323E with Phenyldiazene. A 500-μL sample of 0.5 μM P450 (wild-type CYP4A1, E320A, D323E, E320A/D323E) was reacted with 1 μL of a phenyldiazene stock solution (40 mM methylphenyldiazene carboxylate azo ester in 1 M KOH). The methylphenyldiazene carboxylate azo ester was from Research Organics, Inc. After the reaction, a spectrum from 350 to 600 nm was taken of the protein.

Binding of Substituted Imidazoles to CYP4A1, E320A, D323E, and E320A/D323E. A 500-μL sample of 0.25 μM P450 (wild-type CYP4A1, E320A, D323E, or E320A/D323E) was titrated with imidazole, 1-methylimidazole, 1-phenylimidazole, 1-benzylimidazole, 4-methylimidazole, 4-phenylimidazole, 4,5-dichloroimidazole, 4,5-dibromoimidazole, and 4,5-diphenylimidazole. The difference spectra from 350 to 700 nm were monitored until no further changes were observed.

RESULTS

Expression and Spectroscopic Characterization of Mutant Proteins. The mutations to be made in CYP4A1 were chosen by alignment of its sequence with that of $P450_{BM-3}$, for which a crystal structure is available (*14*). The sequence alignments were done with the GCG, Clustal V, and PIMA alignment programs (*37*, *38*). $P450_{BM-3}$ was chosen for this purpose because it catalyzes the oxidation of fatty acids and is the best model for CYP4A1 among the enzymes of known structure (*39*). The most relevant region of the sequence alignment is shown in Figure 2 with the mutated CYP4A1 residues and the corresponding $P450_{BM-3}$ (CYP102) residues in bold type. The alignment places the polar CYP4A1 residues Glu-320 and Asp-323 on the I-helix close to the heme group and the substrate (Figure 1), so these two residues were targeted for mutagenesis. In each case, the CYP4A1 residue was mutated to the corresponding residue in $P450_{BM-3}$, yielding the E320A, D323E, and E320A/D323E mutants. The mutagenesis was done using the pAlter method, and the mutated cDNAs were sequenced prior to expression to confirm that no errors had been introduced into the sequence.

Wild-type CYP4A1 and each of the mutants was heterologously expressed in *E. coli* with a six-histidine tag on the carboxy terminus to simplify purification of the protein. Comparison of the activity of the wild-type protein with data in the literature (*40*) indicates that the polyhistidine tag does not alter the activity of the protein. The E320A, D323E, and E320A/D323E mutations did not affect the level of expression of the P450 in the cells. The wild type and the three mutants are expressed at a level of 70−120 nmol L^{-1}, as judged by measurements of the P450 chromophore.

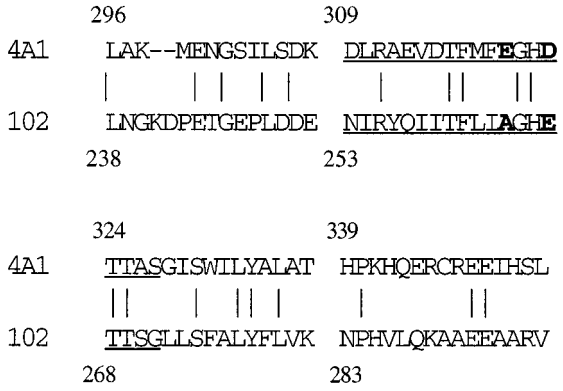

FIGURE 2: Sequence comparison of the pertinent region of CYP4A1 and CYP102. The I-helix of the two proteins is underlined, and identical residues in the two sequences are indicated by a bar. The sequence identity in the I-helix region is 37%, compared to an overall sequence identity of ~25% for the two proteins.

Table 1: Absorption Maxima of CYP4A1 and Three of Its Mutants in the Ferric and Ferrous−CO States

enzyme	Fe^{3+} (nm)	Fe^{2+}−CO (nm)
CYP4A1	418	453
E320A	397, 418	452
D323E	419	452
E320A/D323E	418	452

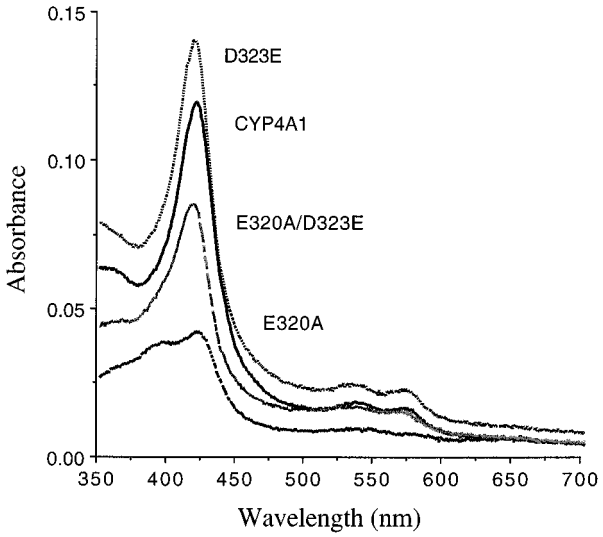

FIGURE 3: Absorption spectra of recombinant CYP4A1 and its E320A, D323E, and E320/D323E mutants. The spectra have been offset for clarity.

The spectrum of the ferrous−CO complex of each of the proteins exhibits a maximum at 452 nm, as expected for an intact P450 enzyme (Table 1) (*35*). The spectrum shows that the P420 content in the wild-type and mutant proteins is very low, on the order of 5−10 nmol L^{-1}, and does not vary among the wild type and the mutants. The P420 is eliminated during the purification procedure. The similarities in the spectra of the ferric (Figure 3) and ferrous−CO complexed proteins indicate that the mutations do not grossly alter the active site structure and heme environment. However, the E320A mutant exhibits a mixed spin state in the

Table 2: Kinetic Constants and Regiospecificities for Lauric Acid Hydroxylation by CYP4A1 and Three of Its Mutants

enzyme	product ratio ω:$\omega-1$	K_m (μM)	V_{max} (min^{-1})	NADPH consumption (nmol min^{-1} nmol^{-1})
CYP4A1	20:1	160 ± 40	150 ± 10	320 ± 20
D323E	10:1	29 ± 9	33 ± 3	320 ± 20
E320A	5:1	36 ± 5	21 ± 2	300 ± 20
E320A/D323E	2:1	31 ± 6	12 ± 1	290 ± 20

Table 3: Spectroscopically Determined K_s Values for the Binding of Substituted Imidazoles to CYP4A1 and Three of Its Mutants

	K_S (mM)			
imidazole[a]	CYP4A1	E320A	D323E	E320A/D323E
Im	1.4 ± 0.1	4 ± 1	1.1 ± 0.2	1.3 ± 0.2
1-MeIm	4.2 ± 0.6	5.1 ± 0.3	2.0 ± 0.6	1.4 ± 0.8
1-PhIm	0.09 ± 0.01	0.09 ± 0.02	0.06 ± 0.01	0.054 ± 0.006
1-BzIm	0.12 ± 0.02	0.15 ± 0.03	0.19 ± 0.08	0.088 ± 0.009
4-MeIm	1.3 ± 0.1	6.2 ± 0.3	1.6 ± 0.3	0.7 ± 0.1
4-PhIm	0.09 ± 0.02	0.10 ± 0.02	0.05 ± 0.01	0.022 ± 0.002
4,5-diClIm	1.4 ± 0.1	0.85 ± 0.01	0.63 ± 0.02	0.36 ± 0.07
4,5-diBrIm	0.10 ± 0.02	1.1 ± 0.3	0.22 ± 0.03	0.19 ± 0.05
4,5-diPhIm	ND	0.9	0.14	0.16

[a] Table abbreviations: Im, imidazole; 1-MeIm, 1-methylimidazole; 1-PhIm, 1-phenylimidazole; 1-BzIm, 1-benzylimidazole; 4-MeIm, 4-methylimidazole; 4-PhIm, 4-phenylimidazole; 4,5-diClIm, 4,5-dichloroimidazole; 4,5-diBrIm, 4,5-dibromoimidazole; 4,5-diPhIm, 4,5-diphenylimidazole.

ferric resting state (Figure 3). In $P450_{BM-3}$ Ala-264 is involved in hydrogen bonding to the axial water ligand and to the conserved Thr-268, two interactions that may influence the Fe spin state of the protein. The mutations do alter the stabilities of the proteins despite the fact that their expression levels are similar to those of the wild type. Thus, the purified wild type and E320A mutant are stable to storage at −70 °C but the purified D323E and E320A/D323E mutants are not stable to such storage in the absence of imidazole. Imidazole helps to stabilize the proteins by coordinating to the heme iron. Despite these differences in stability, the wild-type and mutant proteins were stable during the time course of the experiments reported here.

Catalytic Activities of the Mutants. The wild-type and all three of the mutant proteins catalyze the ω- and ($\omega-1$)-hydroxylation of lauric acid, although differences are observed in the rates of formation and total amounts of the hydroxylated lauric acid products (Table 2). Despite the changes in the rates of lauric acid hydroxylation, the mutations do not significantly alter the rate of NADPH consumption: the wild type and all three mutants consume NADPH at a rate of approximately 300 nmol min^{-1} nmol^{-1} (Table 2). The changes in the rates of lauric acid hydroxylation are thus due to different degrees of uncoupled turnover that result in the reduction of O_2 to H_2O_2 or H_2O (*41*).

Binding of Imidazoles to CYP4A1. To examine the nature of the active site changes wrought by the E320A, D323E, and E320A/D323E mutations, we determined the K_s values for the binding of 1- and 4-substituted imidazoles to each of the proteins (Table 3). The K_s values correspond to spectroscopically determined K_d values and are obtained by measuring the change in the difference spectrum as a function of the inhibitor concentration (Figure 4). As shown in Table 3, the imidazoles generally bind most tightly to the E320A/D323E double mutant, followed by the D323E mutant and the wild type, and bind least tightly to the E320A mutant. With all three enzymes, the 1-phenyl-, 4-phenyl-, and 1-benzylimidazoles bind considerably more tightly than the 1-methyl, 4-methyl, and unsubstituted analogues, as expected from the greater lipophilicity of a phenyl (π = 1.96) or benzyl (π = 2.01) than a methyl (π = 0.56) or hydrogen (π = 0) substituent. With all three enzymes, a 1-Me group decreases inhibitor binding but the effect of a 4-Me is inconsistent, increasing binding to the double mutant, having little effect on binding to the wild type and decreasing binding to the D323E and E320A single mutants. The decreases in binding presumably stem from steric interactions, but the strong increases in binding of the 1-phenyl, 4-phenyl, and 1-benzyl analogues show that lipophilicity is more important than the steric constraints. The binding of substituted imidazoles, as found with other P450 enzymes (*42*), is related to their lipophilicity, but the fact that the E320A/D323E double mutant more readily accommodates large ligands suggests that its active site is less sterically constrained.

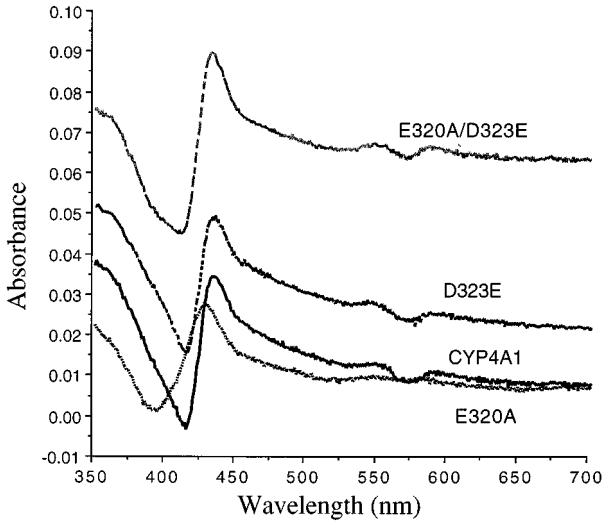

FIGURE 4: Difference spectra obtained for the binding of 4-phenylimidazole (25 mM) to CYP4A1 and its E320A, D323E, and E320/D323E mutants.

Reaction with Phenyldiazene. The wild-type and the three mutant proteins were incubated with phenyldiazene (PhN═NH), an agent that has been extensively used to probe the active site topologies of P450 enzymes and nitric oxide synthases (*32*, *43*). The reaction of phenyldiazene with hemoproteins with an open iron coordination site commonly yields a stable σ-bonded phenyl−iron complex (Fe−Ph). If the proximal iron ligand is a thiolate anion, the phenyl−iron complex gives rise to an absorption maximum at 475−480 nm. However, the reaction of phenyldiazene with wild-type CYP4A1 and the three mutants does not give a spectroscopically detectable phenyl−iron complex. The only spectroscopically observable change is a slow decrease in the intensity of the Soret maximum of the protein, as shown in Figure 5 for the reaction with the E320A/D323E mutant. The failure of CYP4A1 to react with phenyldiazene to give a phenyl−iron complex suggests that the active site is sterically constrained and that the steric constraints that prevent complex formation are not relieved by the mutations.

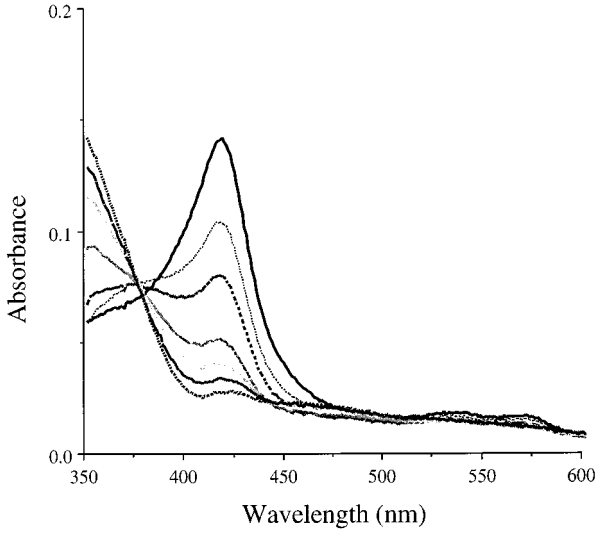

FIGURE 5: Absorption spectrum of E320A/D323E CYP4A1 incubated with 1.4 mM phenyldiazene. The spectra, from top to bottom at 418 nm, were recorded after incubation with phenyldiazene for 0, 5, 10, 15, 20, 25, and 30 min.

Table 4: Inactivation of CYP4A1-Catalyzed Lauric Acid Hydroxylation by Preincubation with 10 MM 1-ABT for 20 min under Turnover Conditions ($n = 3 \pm 1$)

		act. after preincubn (min^{-1})	
enzyme	act. with 1-ABT but no preincubn (min^{-1})	without 1-ABT	with 1-ABT
CYP4A1	62 ± 4	59 ± 3	53 ± 6
E320A	12 ± 2	10 ± 1	9 ± 1
D323E	15 ± 3	13 ± 2	6 ± 1
E320A/D323E	9 ± 2	6 ± 1	4 ± 0.5

Inactivation by 1-ABT. Wild-type CYP4A1 and the three mutants are differentially affected by incubation with 1-ABT, a mechanism-based P450 inactivating agent (*29*, *30*). A 10 mM concentration of 1-ABT has little effect on lauric acid hydroxylation by either the wild type or the E320A mutant, but the activities of both the D323E and E320A/D323E mutants are inhibited (Table 4). The activity of the D323E mutant decreases by 50% and that of the E320A/D323E by 25% when preincubated with 1-ABT under turnover conditions. A detailed analysis of the incubation of wild-type and D323E CYP4A1 with 1-ABT clearly establishes that there is little time-dependent loss of wild-type activity (Figure 6). The very minor background loss of wild-type activity with time is almost certainly due to thermal inactivation during the 30-min assay period. However, the loss of the activity of the D323E mutant shows a linear dependence between the log of the activity and the incubation time (Figure 6) and is 1-ABT dependent (Table 4). According to CO difference spectra, in neither case is the heme or the cysteine thiolate−Fe bond destroyed because the intensity of the normal ferrous−CO absorption maximum at 452 nm is not decreased, as shown for the D323E mutant in Figure 7. These results indicate that the purified wild-type enzyme is not susceptible to direct inactivation by 1-ABT despite the fact that the fatty acid ω-hydroxylase activity can be inactivated by this inhibitor both in vivo and in microsomal preparations (*22*, *25*−*28*). However, the D323E CYP4A1 mutant is directly inactivated by 1-ABT.

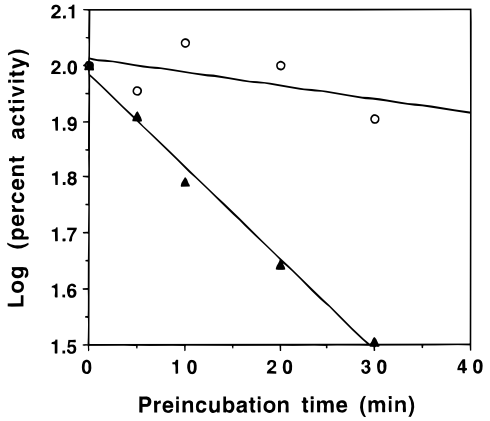

FIGURE 6: Time dependence of the loss of the catalytic activity of the wild-type (○) and D323E (▲) CYP4A1. The log of the percent activity is plotted versus the time of preincubation with 10 mM 1-ABT. The absolute value for the activity at time zero for the wild-type enzyme was 100 ± 20 min^{-1} and for the D323E mutant was 16 ± 2 min^{-1}.

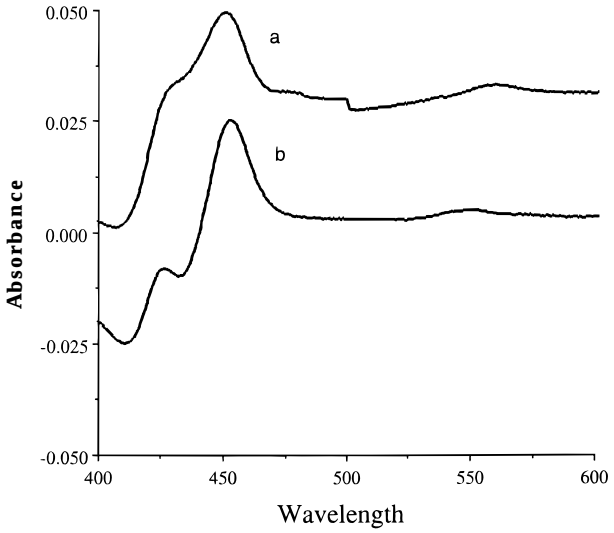

FIGURE 7: Absorption spectrum of the ferrous−CO complex of D323E CYP4A1 before (a) and after (b) preincubation with 10 mM 1-ABT under turnover conditions.

DISCUSSION

Relatively little information is available on the active site structures of the CYP4A family of P450 enzymes, including CYP4A1, the most extensively studied member of the group. Studies of the substrate specificity of CYP4A1, and of the binding of inhibitors of different chain lengths to it (*8*), provide some information on the relationship between the carboxyl terminus and the site of oxidation on the substrate but shed no light on either the amino acid residues that determine the substrate specificity or the mechanism by which the thermodynamically disfavored ω-hydroxylation is promoted over the favored (ω−1)-hydroxylation. No site-specific mutagenesis studies have been reported for the CYP4A1 class of enzymes that explore these or other questions.

Two residues, Glu-320 and Asp-323, have been shown in the present study to directly influence the active site structure and the ω- versus (ω−1)-hydroxylation specificity of CYP4A1. Mutation of Glu-320 to an alanine, Asp-323 to a glutamic acid, or simultaneous mutation of both residues yields proteins with spectroscopic and physical properties

comparable to those of the wild-type enzyme, although the E320A mutation causes a change in the proportion of high to low spin state of the ferric protein (Figure 3). In particular, the ferrous−CO difference spectrum of the proteins confirms that, in each case, the iron retains the proximal thiolate ligand (Table 1). These results indicate that the mutations do not grossly disrupt the active site structure, although the increased thermal lability of the mutant proteins demonstrates that the mutations do have some impact on the overall protein structure. The general structural effect is minor, however, because the proteins are catalytically active. Comparison of the K_m values of the three mutants with wild-type CYP4A1 shows that all three mutations increase the affinity for lauric acid about 5-fold (Table 2). The increase in the affinity does not depend on whether a negative charge is lost, as in the E320A mutant, or simply relocated, as in the D323E mutant. The decreased K_m values, and their independence from the nature of the side-chain modification, are consistent with an expansion of the active site cavity that facilitates binding of the fatty acid.

In contrast to the binding affinities, the V_{max} values of the mutants are lower than those of the wild-type enzyme. The D323E mutation decreases the V_{max} by approximately 5-fold, the E320A mutation 7−8-fold, and the double mutation greater than 10-fold. These decreases in the rate of lauric acid hydroxylation are not due to decreases in the ability of the enzymes to accept electrons from P450 reductase, or in their ability to activate molecular oxygen, because the rate of NADPH consumption is not significantly altered by the mutations (Table 2). Thus, the decrease in lauric acid hydroxylation is due to an increase in the uncoupled reduction of oxygen to H_2O_2 and/or water. It is therefore clear that Glu-323 and Asp-320 contribute significantly to the coupling of NADPH and O_2 consumption to the oxidation of fatty acid substrates.

The consequences of the mutations extend to the regiochemistry of lauric acid hydroxylation. Whereas the wild-type enzyme favors ω- over (ω−1)-hydroxylation by a ratio of 20:1, this preference decreases to 10:1 in the D323E mutant, 5:1 in the E320A mutant, and only 2:1 in the E320A/D323E double mutant (Table 2). Thus, the two mutations together bring about an order of magnitude change in the regiospecificity of the enzyme. This finding, supported by the evidence for increased uncoupled turnover (Table 2), establishes that Glu-323 and Asp-320 are located within the active site of the protein, or in positions that allow them to perturb residues that are. In view of the thermodynamic preference for (ω−1)- versus ω-oxidation, the mutations appear to loosen the active site constraints that enforce the ω-hydroxylation specificity. We have previously suggested that steric constriction within the active site in the vicinity of the ferryl oxygen may be a key mechanism used by the enzyme to promote the disfavored ω-hydroxylation (*11*). The progressive decrease in the ω-hydroxylase specificity in traversing the D323E, E320A, and E320A/D323E mutants suggests that the mutations increasingly fluidize the active site, relax the steric constraints that control the reaction regiospecificity, and uncouple the catalytic turnover from fatty acid oxidation (Table 2).

In a search for independent evidence that the mutations make the active site more accessible to exogenous ligands, we examined the reactions of the wild-type and mutant CYP4A1 enzymes with phenyldiazene. However, phenyldiazene reacts as slowly with the three mutants as it does with the wild-type enzyme and does not give rise with any of the proteins to the 478-nm absorption characteristic of a phenyl−iron complex (Figure 5). This finding indicates that the active site in the vicinity of the iron is so sterically constrained that the phenyl−iron complex is not formed or is formed transiently. The crystal structure of the $P450_{cam}$ phenyl−iron complex shows that the complex requires an absolute minimum of 5.7 Å of headspace directly above the iron atom, as this is the height to which the phenyl group extends above the iron (*44*, *45*). Although the proteins do not form a phenyl−iron complex, they react with phenyldiazene, or products of its decomposition, in a manner that results in slow degradation of the prosthetic heme group to undefined products. These results indicate that the active site steric barriers are not sufficiently loosened by mutations to permit assembly of the phenyl−iron complex.

The binding of substituted imidazoles to CYP4A1 provides an additional probe of the active site structure. The spectroscopic studies establish that the imidazoles coordinate to the heme iron atom (Figure 4), although complex formation could involve a noncatalytic conformation of the protein. That is, the imidazoles could coordinate to a conformation of the protein in which the substrate access channel remains open rather than closed. Despite this limitation, the binding of the imidazoles provides a measure of the properties of the active site. The relative K_s values measured here suggest that the D323E and particularly the E320A/D323E active sites more readily accommodate large ligands, and are therefore effectively larger, than those of the wild type or E320A mutant.

Further evidence that the wild-type active site is highly constrained in the vicinity of the iron is provided by the inability of 1-ABT to inactivate CYP4A1. Oxidation of 1-ABT by cytochrome P450 results in the formation of benzyne, which in some P450 enzymes adds across two of the heme nitrogen atoms to give a bis-*N*-aryl heme adduct (*29*,*30*), while in others it appears to bind covalently to active site residues (*31*). However, as shown here, neither purified CYP4A1 nor its E320A mutant is significantly inactivated by 1-ABT (Table 4, Figure 6). In contrast, the D323E mutant and, to a lesser extent, the E320A/D323E double mutant are inactivated in a time- and turnover-dependent manner by 1-ABT (Table 4, Figure 6). The D323E, but not the E320A, mutation opens the active site sufficiently to allow the oxidation of 1-ABT and the subsequent reaction of the benzyne that is formed with the protein. This finding is consistent with the conclusion from the studies of the binding of substituted imidazoles that the D323E mutation opens the active site to a larger extent than the E320A mutation (vide supra). Spectroscopic quantitation of the D323E ferrous−CO complex before and after the reaction with 1-ABT indicates that the inactivation does not result in the loss of the heme chromophore and therefore is likely to involve covalent modification by the reactive intermediate of one or more protein residues (Figure 7).

[2] Incubation of recombinant CYP4A1 with uninduced rat liver microsomes or purified recombinant CYP3A4 in the presence of 1-ABT under turnover conditions did not result in increased loss of the CYP4A1 activity.

The finding that 1-ABT does not inactivate purified CYP4A1 is surprising in view of the fact that 1-ABT has been shown in several studies to suppress the hepatic ω-hydroxylase activity (*22*, *26*−*29*). The possibility that the polyhistidine tail perturbs the ability of the recombinant enzyme to interact with 1-ABT is obviated by the finding that CYP4A1 purified from clofibrate-induced rat liver is similarly insensitive to inactivation by 1-ABT (C. CaJacob and P. R. Ortiz de Montellano, unpublished results). One possibility is that inactivation of CYP4A1 in microsomal preparations and in vivo requires the intervention of an additional, unidentified factor that is lost on purification of the enzyme.[2] It is interesting to note in this context that a similar finding has been made with respect to the ability of 1-ABT to suppress P450-dependent adrenal sterol metabolism (*46*). Studies with guinea pigs have shown that $P450_{scc}$ and the 11-, 17-, and 21-sterol hydroxylases are not inactivated in vitro by 1-ABT even though these activities are suppressed in vivo by this agent. To explain these results, it was postulated that an extra-adrenal metabolic step was required for the inhibition to be observed. Nevertheless, if a hepatic factor is required to enable the inactivation of CYP4A1 and the sterol hydroxylases by 1-ABT, it is not a universal requirement because direct inactivation of some P450 isoforms by 1-ABT is observed (*47*, *48*). An alternative possibility is that 1-ABT effectively inactivates CYP4A2 and CYP4A3 but not CYP4A1, and that the loss of hepatic ω-hydroxylase activity observed in earlier studies with 1-ABT was due to selective inactivation of a subset of the CYP4A group of enzymes.

In sum, the present studies establish that Glu-320 and Asp-323 are part of the CYP4A1 active site, are among the residues that define the steric environment of the heme group, partially determine both the degree of coupled turnover and the regiospecificity of fatty acid hydroxylation, and control the susceptibility of the enzyme to inactivation by at least one mechanism-based inhibitor. The two residues thus appear to occupy positions analogous to those of the corresponding residues in $P450_{BM-3}$ (Figure 1).

ACKNOWLEDGMENT

We thank Ronald Estabrook for kindly providing the CYP4A1 cDNA and Stephen M. Black for the cytochrome P450 reductase and cytochrome b_5 cDNAs.

REFERENCES

1. Simpson, A. E. C. M. (1997) *Gen. Pharmacol. 28*, 351−359.
2. Kupfer, D. (1980) *Pharmacol. Ther. 11*, 469−496.
3. Kimura, S., Hardwick, J. P., Kozak, C. A., and Gonzalez, F. J. (1989) *DNA 8*, 517−525.
4. Stromstedt, M., Hayashi, S., Zaphiropoulos, P. G., and Gustafsson, J. A. (1990) *DNA Cell Biol. 9*, 569−577.
5. Kroetz, D. L., Huse, L. M., Thuresson, A., and Grillo, M. P. (1997) *Mol. Pharmacol. 52*, 362−372.
6. Amet, Y., Berthou, F., Goasduff, T., Salaun, J. P., Le Breton, L., and Menez, J. F. (1994) *Biochem. Biophys. Res. Commun. 203*, 1168−1174.
7. Castle, P. J., Merdink, J. L., Okita, J. R., Wrighton, S. A., and Okita, R. T. (1995) *Drug Metab. Dispos. 23*, 1037−1043.
8. Fukuda, T., Imai, Y., Komori, M., Nakamura, M., Kusunose, E., Satouchi, K., and Kusunose, M. (1994) *J. Biochem. (Tokyo) 115*, 338−344.
9. Aoyama, T., Hardwick, J. P., Imaoka, S., Funae, Y., Gelboin, H. V., and Gonzalez, F. J. (1990) *J. Lipid Res. 31*, 1477−1482.
10. Powell, P. K., Wolf, K., and Lasker, J. M. (1996) *Arch. Biochem. Biophys. 335*, 219−226.
11. Cajacob, C. A., Chan, W., Shephard, E., and Ortiz de Montellano, P. R. (1988) *J. Biol. Chem. 263*, 18640−18649.
12. Poulos, T. L., Finzel, B. C., and Howard, A. J. (1987) *J. Mol. Biol. 195*, 687−700.
13. Hasemann, C. A., Ravichandran, K. G., Peterson, J. A., and Deisenhofer, J. (1994) *J. Mol. Biol. 236*, 1169−1185.
14. Ravichandran, K. G., Boddupalli, S. S., Hasemann, C. A., Peterson, J. A., and Deisenhofer, J. (1993) *Science 261*, 731−736.
15. Cupp-Vickery, J. R., and Poulos, T. L. (1995) *Nature Struct. Biol. 2*, 144−153.
16. Miura, Y., and Fulco, A. J. (1975) *Biochim. Biophys. Acta 388*, 305−317.
17. Li, H., and Poulos, T. L. (1997) *Nat. Struct. Biol. 4*, 140−146.
18. Oliver, C. F., Modi, S., Sutcliffe, M. J., Primrose, W. U., Lian, L.-Y., and Roberts, G. C. K. (1997) *Biochemistry 36*, 1567−1572.
19. Modi, S., Sutcliffe, M. J., Primrose, W. U., Lian, L.-Y., and Roberts, G. C. K. (1996) *Nat. Struct. Biol. 3*, 414−417.
20. Lu, P., Alterman, M. A., Chaurasia, C. S., Bambal, R. B., and Hanzlik, R. P. (1997) *Arch. Biochem. Biophys. 337*, 1−7.
21. Ellin, A., and Orrenius, S. (1975) *FEBS Lett. 50*, 378−381.
22. Romano, M. C., Straub, K. M., Yodis, L. A. P., Eckhardt, R. D., and Newton, J. F. (1988) *Anal. Biochem. 170*, 83−93.
23. Ortiz de Montellano, P. R., and Correia, M. A. (1995) in *Cytochrome P450: Structure, Mechanism, and Biochemistry* (Ortiz de Montellano, P. R., Ed.) 2nd ed., pp 305−364, Plenum Press, New York.
24. Bambal, R. B., and Hanzlik, R. P. (1996) *Arch. Biochem. Biophys. 334*, 59−66.
25. Ortiz de Montellano, P. R., and Reich, N. O. (1984) *J. Biol. Chem. 259*, 4136−4141.
26. Reich, N. O., and Ortiz de Montellano, P. R. (1986) *Biochem. Pharmacol. 35*, 1227−1233.
27. Ortiz de Montellano, P. R., and Costa, A. K. (1986) *Arch. Biochem. Biophys. 251*, 514−524.
28. Kaikaus, R. M., Chan, W. K., Lysenko, N., Ray, R., Ortiz de Montellano, P. R., and Bass, N. M. (1993) *J. Biol. Chem. 268*, 9593−9603.
29. Ortiz de Montellano, P. R., Mathews, J. M., and Langry, K. C. (1984) *Tetrahedron 40*, 511−519.
30. Ortiz de Montellano, P. R., and Mathews, J. M. (1981) *Biochem. J. 195*, 761−764.
31. Knickle, L. C., Woodcroft, K. J., Webb, C. D., and Bend, J. R. (1991) *FASEB J. 5*, A479.
32. Ortiz de Montellano, P. R. (1995) *Biochimie, 77*, 581−593.
33. Fisher, C. W., Shet, M. S., Caudle, D. L., Martin-Wixtrom, C. A., and Estabrook, R. W. (1992) *Proc. Natl. Acad. Sci. U.S.A. 89*, 10817−10821.
34. Muchmore, D. C., McIntosh, L. P., Russell, C. B., Anderson, D. E., and Dalqhuist, F. W. (1989) *Methods Enzymol. 177*, 44−73.
35. Omura, T., and Sato, R. (1964) *J. Biol. Chem. 239*, 2370−2378.
36. Holmans, P. L., Shet, M. S., Martin-Wixtrom, C. A., Fisher, C. W., and Estabrook, R. W. (1994) *Arch. Biochem. Biophys. 312*, 554−565.
37. Higgins, D. G., Bleasby, A. J., and Fuchs, R. (1992) *Comput. Appl. Biosci. 8*, 189−191.
38. Smith, R. F., and Smith, T. F. (1992) *Protein Eng. 5*, 35−41.
39. Fulco, A. J. (1991) *Annu. Rev. Pharmacol. Toxicol. 31*, 177−203.
40. Shet, M. S., Fisher, C. W., Holmans, P. L., and Estabrook, R. W. (1996) *Arch. Biochem. Biophys. 330*, 199−208.

41. Archakov, A. I., and Bachmanova, G. I. (1990) *Cytochrome P-450 and Active Oxygen* pp 129−138, Taylor & Francis, New York.
42. Wilkinson, C. F., Hetnarski, K., Cantwell, G. P., and DiCarlo, F. J. (1974) *Biochem. Pharmacol. 23*, 2377−2386.
43. Gerber, N. C., Rodriguez-Crespo, I., Nishida, C. R., and Ortiz de Montellano, P. R. (1997) *J. Biol. Chem. 272*, 6285−6290.
44. Raag, R., Swanson, B. S., Poulos, T. L., and Ortiz de Montellano, P. R. (1990) *Biochemistry*, *29*, 8119−8126.
45. Tuck, S. F., and Ortiz de Montellano, P. R. (1992) *Biochemistry 31*, 6911−6916.
46. Xu, D., Voigt, J., Mico, B., and Colby, H. (1995) *J. Steroid Biochem. Mol. Biol. 54*, 281−285.
47. Ortiz de Montellano, P. R., Mico, B. A., Mathews, J. M., Kunze, K. L., Miwa, G. T., and Lu, A. Y. H. (1981) *Arch. Biochem. Biophys. 210*, 717−728.
48. Grimm, S. W., Bend, J. R., and Halpert, J. R. (1995) *Drug Metab. Dispos. 23*, 577−583.

BI972458S